Numerical study on the measurement of thin film mechanical properties by means of nanoindentation

Xi Chen and Joost J. Vlassak[a)]
Division of Engineering and Applied Sciences, Harvard University, Cambridge, Massachusetts 02138

(Received 6 March 2001; accepted 30 July 2001)

Nanoindentation is a technique commonly used for measuring thin film mechanical properties such as hardness and stiffness. In this study, we used the finite element method to investigate the effect of substrate and pileup on hardness and stiffness measurements of thin film systems. We define a substrate effect factor and construct a map that may be useful in the interpretation of indentation measurements when it is not possible to make indentations shallow enough to avoid the influence of the substrate on the measurements. A new technique for measuring mechanical properties of thin films by nanoindentation is suggested at the end of this article.

I. INTRODUCTION

One of the most important material configurations in microelectronics, optoelectronics, and thermal barrier coating technology consists of a coating material deposited onto a substrate of another material. Proper measurement of the mechanical properties of thin films is the first step in analyzing the mechanics of thin films and multilayers. Industry has long relied on indentation techniques for measuring the hardness and stiffness of a wide range of bulk materials. Recently, low-load and depth-sensing indentation, commonly referred to as nanoindentation, has been used to study the mechanical properties of thin films on substrates.[1–4] Nanoindentation experiments can be performed quickly and do not require removal of the film from its substrate. Nanoindentation has been proven particularly useful in measuring the hardness and stiffness of thin films. In general, indentations with contact depths of less than 10% to 20% of the film thickness are needed in order to obtain intrinsic film properties and to avoid the so-called substrate effect.[5] This is often not practical as the thickness of films used in many applications continues to decrease. For example, the thickness of barrier films currently used in semiconductor devices is well below 50 nm and the film stack thickness used for magnetic data storage is less than 100 nm.[3] Due to experimental equipment limitations, it is very difficult to perform indentation tests at such a shallow indentation depth, and it seems that in these cases it is inevitable for the substrate to affect the final measurements.

Several analytical approaches have been developed for measuring mechanical properties such as elastic modulus and yield stress from indentation load-displacement data of a bulk material.[1,2] The equations used to extract the hardness H and indentation modulus M are

$$H = P/A = c_b \sigma_y \quad , \tag{1}$$

and

$$S = \beta \frac{2}{\sqrt{\pi}} M \sqrt{A} \quad , \tag{2}$$

where we have neglected the finite compliance of the measuring system and the indenter tip. The indentation modulus is given by the plane-strain modulus, $E/(1-\nu^2)$, for isotropic materials and by a more complicated weighted average of the elastic constants for anisotropic materials.[6,7] Here, the hardness H is defined as the ratio between indentation load P and projected contact area A, and the contact stiffness $S = dP/d\delta$ is obtained from the elastic unloading curve. The yield stress and Poisson's ratio of the bulk material are σ_y and ν, respectively. The constant c_b in Eq. (1) is a constraint factor[8] that depends on indenter shape and material properties and β is a correction factor that depends on indenter shape, with $\beta = 1$ for axisymmetric indenters and $\beta = 1.03$–1.05 for indenters with square or rectangular cross sections.[7,9] These theories, however, cannot be applied directly to thin film systems. Recently, many experimental and analytical efforts[3,4,10–19] have been made to measure the hardness and stiffness of a thin film in the presence of a substrate. Most of these studies have focused on a limited number of thin film systems and a complete examination

a)Address all correspondence to this author.
e-mail: vlassak@esag.harvard.edu

of the substrate effect on hardness and stiffness measurements of all possible thin film configurations remains yet to be developed.

How deep can an indentation be in order to measure substrate-independent hardness and stiffness? At a given indentation depth, what does one really measure? How do the stiffness and yield strength ratios between the film and substrate affect nanoindentation measurement? In this study, the finite element method (FEM) is used to investigate the effect of the substrate on hardness and stiffness measurements for a variety of thin film systems. The FEM is useful for this purpose because it provides a convenient way of measuring the projected contact area between indenter and material needed for calculation of hardness and stiffness. It is straightforward to vary materials properties over a wide range and the analysis also provides direct information on pile-up height through analysis of the surface contour during the indentation process. The results of this study are useful when analyzing data from indentations that are not shallow enough to avoid the influence of the substrate.

II. MODEL DESCRIPTION

For the purpose of this study, it is convenient to define a bulk material as being soft if indentation causes pile-up around the indenter, and hard when sink-in is present. Whether a material is hard or soft according to this definition, depends of the yield strain, σ_y/E, and the strain-hardening behavior of the material as well as on the indenter geometry. A more quantitative distinction between soft and hard bulk materials will be made in Sec. III. For thin film systems, the system produces pile-up or sink-in depending on the hardness ratio between film and substrate. Figure 1 shows a schematic depiction of pile-up or sink-in for both bulk materials and thin films.

The models for bulk material indentation and thin film indentation are shown in Fig. 2 and Fig. 3, respectively. The indenter is a rigid cone with a half apex angle of $\alpha = 70.3°$, so that the ratio of cross-sectional area to depth is the same as for a Berkovich or Vickers indenter. A static indentation load P is applied to drive the indenter into the bulk material, which is modeled as an elastic–plastic half-space. The bulk material is isotropic and homogeneous, with Young's modulus E, Poisson's ratio ν, yield stress σ_y, and power-law hardening coefficient n (where the uniaxial stress–strain relation is $\epsilon = \sigma/E$ when $\sigma \leq \sigma_y$ and $\epsilon = B\sigma^n$ when $\sigma > \sigma_y$, and B is a material constant). The contact radius is a and the indentation depth is δ. We define the pile-up height as δ_p, so that the projected contact area is given by

$$A = \pi a^2 = \pi(\tan\alpha)^2\,\delta_c^2 = 24.5\delta_c^2 \quad , \tag{3}$$

where

$$\delta_c = \delta + \delta_p \quad . \tag{4}$$

The pile-up height as defined in Eq. (4) contains contributions of both plastic pile-up around the indenter and elastic sink-in, which is counted negative. It is obvious from Eqs. (3) and (4) that the projected contact area depends on the pile-up height δ_p. Oliver and Pharr[2]

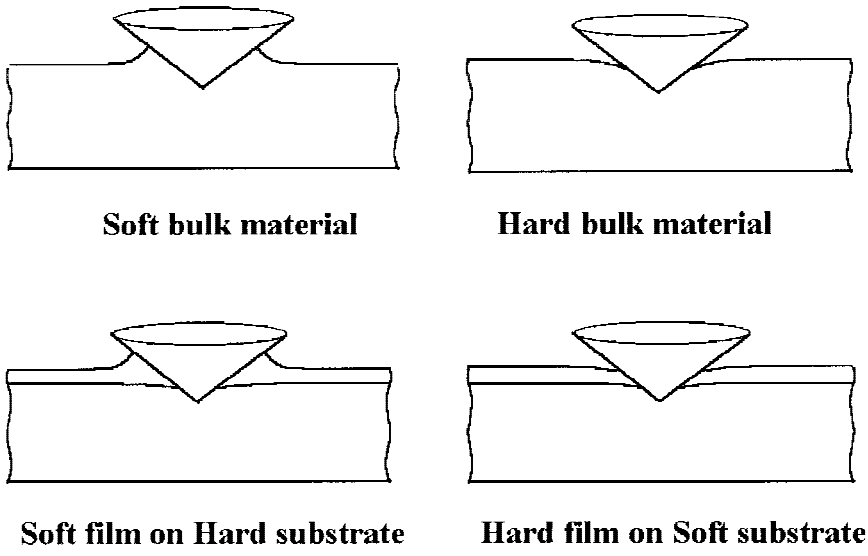

FIG. 1. Cartoons of nanoindentation on bulk materials and thin films.

proposed a model for determining the contact area in which plastic pileup is neglected. According to this model, the amount of elastic sink-in is given by

$$|\delta_p| = \epsilon \frac{P_{\max}}{S_{\max}} \quad , \tag{5}$$

where $\epsilon = 0.75$ for a conical indenter. The hardness is then obtained from Eq. (1) and the stiffness can be derived from Eq. (2) and the load-displacement curve of the unloading process.

Figure 3 shows our model for nanoindentation in thin films. The film thickness is h and the substrate is infinitely deep. The subscripts s and f are used to denote the material properties of the substrate and film, respectively. Both the film and substrate are homogeneous and isotropic.

Since recent work by Mesarovic and Fleck[20] has shown that Poisson's ratio is a minor factor for static indentations, we let $\nu = 0.3$ for bulk materials and $\nu_f = \nu_s = 0.3$ for thin film systems in this study. To further simplify the model, we focus on elastic–perfectly plastic materials by taking $n \to \infty$ for the bulk material, along with $n_f \to \infty$ and $n_s \to \infty$ for thin films.

Finite element calculations were performed using the commercial code ABAQUS[21] on Sun workstations. The rigid contact surface option was used to simulate the rigid indenter and the option for finite deformation and strain was employed. A typical mesh for the axisymmetric indentation model comprises more than 5000 8-node elements. As already mentioned, the substrate material is taken to be elastic–perfectly plastic, with a von Mises surface to specify yielding. The Coulomb's friction law is used between contact surfaces and the friction coefficient is taken to be 0.1, which is also a minor factor for nanoindentation.[20] The projected contact area is calculated directly from the numerical results by analyzing the nodes in contact with the indenter.

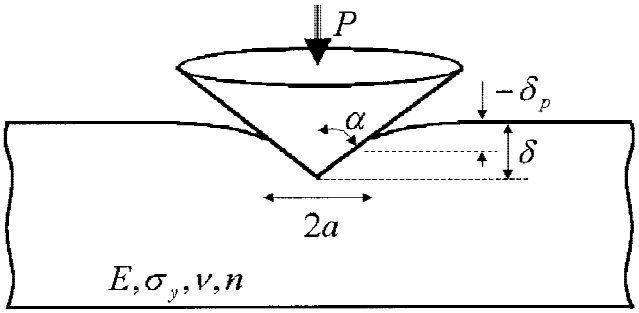

FIG. 2. Model description for indentation on a bulk material.

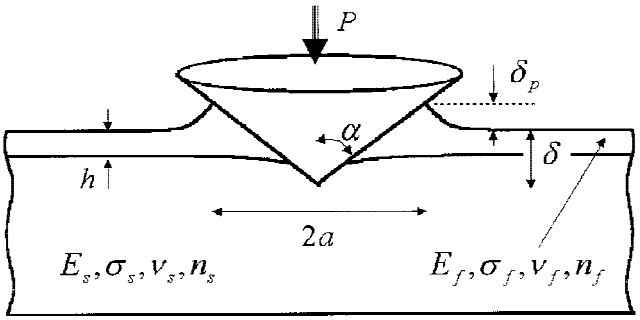

FIG. 3. Model description for indentation on a film/substrate composite.

III. INDENTATION ON BULK MATERIALS

In this section, the classical formulas for bulk materials, Eqs. (2) and (5), are reexamined and compared to the results obtained from finite element simulations. The constraint factor c calculated from the FEM program is plotted in Fig. 4 as a function of $E \tan \beta_0/\sigma_y$ (where $\beta_0 = 90° - \alpha$) for a variety of materials ranging from very hard to very soft and this functional dependence is compared with the theoretical result by Johnson.[8] It can be seen that the FEM results are in good agreement with the theoretical analysis. The constraint factor c is about 3 when $E \tan \beta_0/\sigma_y > 100$ and it decreases when the bulk material gets harder.

The height of the pile-up resulting from the indentation, δ_p, changes linearly with the indentation depth δ, an observation that agrees well with experimental evidence for work-hardened copper.[22] The ratio δ_p/δ calculated using finite elements is plotted against $E \tan \beta_0/\sigma_y$ and compared with the Oliver–Pharr prediction [Eq. (5)] in

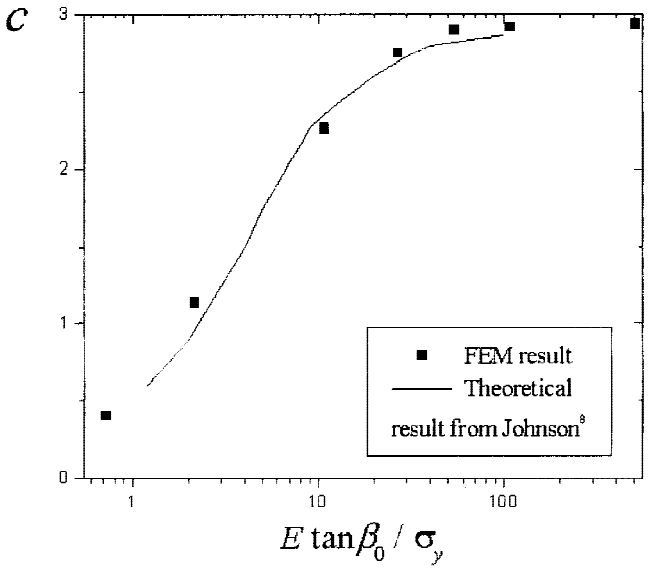

FIG. 4. The constraint factor c as a function of the normalized yield strain of the bulk material.

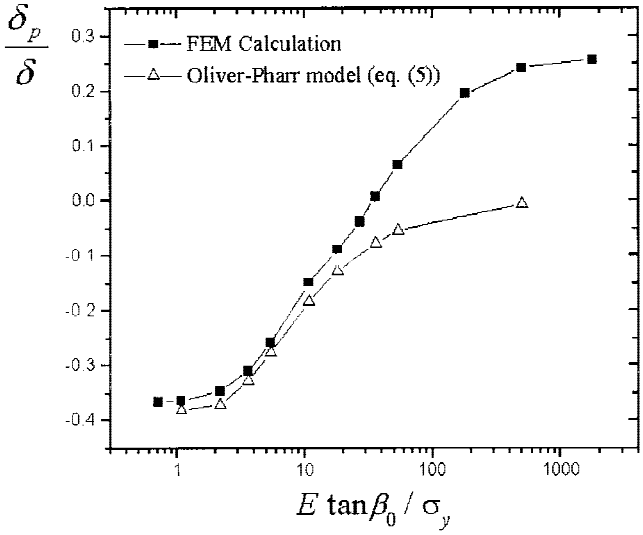

FIG. 5. Plot of the normalized height of pile-up as a function of the yield strain.

Fig. 5. The figure shows that the ratio δ_p/δ has a lower limit of −0.36 and an upper limit of 0.26. The lower limit corresponds to the case where the indentation is purely elastic. This is consistent with the theoretical solution by Harding and Sneddon,[23] who found the following relationship between contact radius a and indentation depth δ:

$$a = \frac{2}{\pi}\delta \tan \alpha \quad , \tag{6}$$

for the elastic contact of a cone on a half space. The amount of sink-in for an elastic indentation in a bulk is then

$$\frac{|\delta_p|}{\delta} = 1 - \frac{a}{\delta \tan \alpha} = 1 - \frac{2}{\pi} = 0.36 \quad , \tag{7}$$

independent of the indenter angle. It is now convenient to define a soft or hard material as one for which $E \tan \beta_0/\delta_y > 36$ (where δ_p is positive), or $E \tan \beta_0/\sigma_y < 36$ (where δ_p is negative), respectively. Figure 5 shows that there is very good agreement between the Oliver–Pharr model and the finite element results when the bulk material is hard, but that the model cannot be applied to indentations in soft materials. The discrepancy between the Oliver–Pharr model and the FEM results for large values of $E \tan \beta_0/\sigma_y$ is of course due to pile-up of material around the indenter. The results in Fig. 5 also show that neglecting plastic pile-up may result in an underestimation of the contact area by as much as 66%.

The elastic modulus of the bulk material is calculated using Eq. (2) using the contact stiffness and the projected contact area from a finite element simulation of the unloading process. We find that for both hard and soft materials, Eq. (2) overestimates Young's modulus by approximately 8%. In fact, this is consistent with recent work by Hay *et al.*,[24] where through a theoretical approach they suggested that a correction factor γ should be added to Eq. (2):

$$S = \gamma\beta \frac{2}{\sqrt{\pi}} \frac{E}{1-\nu^2}\sqrt{A} \quad , \tag{8}$$

where

$$\gamma = \pi \frac{\pi/4 + 0.155 \cot \alpha \cdot \dfrac{1-2\nu}{4(1-\nu)}}{\left[\pi/2 - 0.831 \cot \alpha \cdot \dfrac{1-2\nu}{4(1-\nu)}\right]^2} \quad , \tag{9}$$

for a conical indenter. Equation (9) yields $\gamma \approx 1.09$ for $\nu = 0.3$, in good agreement with the FEM results.

IV. INDENTATION IN THIN FILMS

As shown in Sec. III, the Oliver–Pharr model[2] can only be used effectively when the indentation does not produce plastic pile-up. For the case of a soft film on a hard substrate, the hard substrate prevents the soft film material from flowing downwards and thus increases the degree of pile-up (c.f. Fig. 1). Therefore, the Oliver–Pharr model may overestimate the hardness significantly.[14] The presence of the substrate in a hard film–soft substrate composite, on the other hand, enhances the sink-in effect (c.f. Fig. 1) since the plastic region in the soft substrate is much larger than that in the hard film and the substrate is unable to support the large indentation load.[15] Consequently, the Oliver–Pharr model may also be inadequate for this case. This necessitates an extensive FEM study of the hardness and stiffness measurements for a wide range of film-substrate properties.

We have analyzed a wide range of film and substrate systems with materials varying from very hard and stiff to very low and compliant. The hardness of a film on a substrate is calculated from the finite element analysis as a function of normalized indentation depth δ/h, and for different values of σ_f/σ_s and E_f/E_s. This hardness value is then normalized by the hardness H_b of a bulk material with the same yield stress and stiffness as the film. Selected numerical results are shown in Figs. 6(a) to 6(d). When the yield stress of the film is smaller than that of the substrate, it can be seen from Fig. 6(a) that the normalized hardness is constant when $\delta/h < 0.5$. This implies that for the case of a soft film on a hard substrate one may obtain the intrinsic film hardness directly from Eq. (1) as long as the indentation depth is less than 50% of the film thickness. This is due to the fact that plastic zone caused by the indentation is very localized: At indentation depths less than one half of the film thickness, the indenter has yet to feel the effect from the hard substrate and this is equivalent to the indentation of a bulk material. The substrate effect only comes into play when the indentation depth is larger than one half of the film

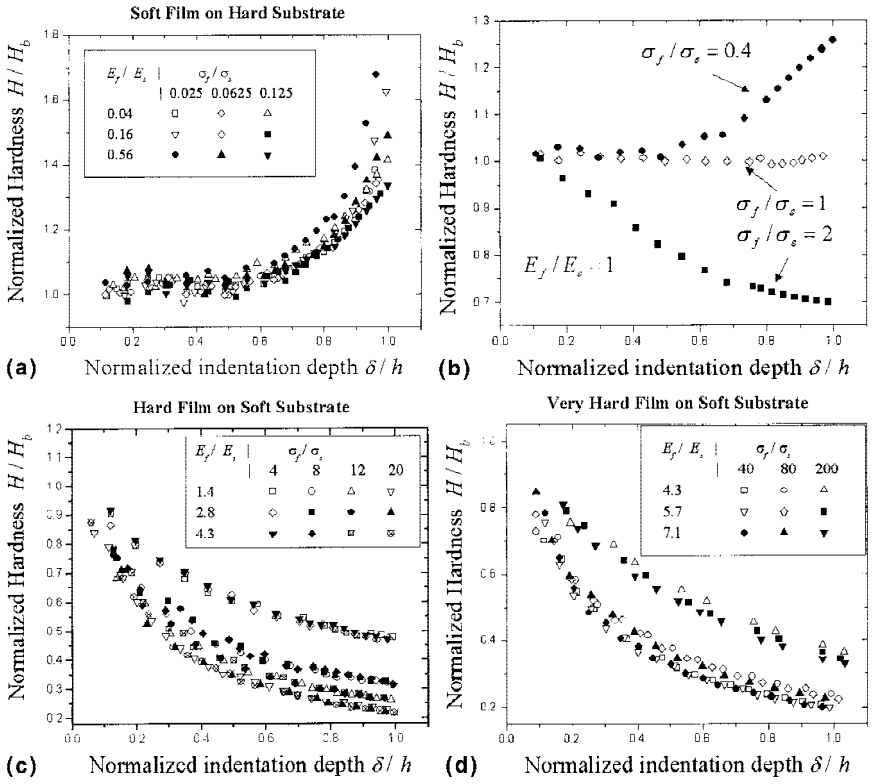

FIG. 6. Variation of the normalized film hardness *H/Hb* with normalized indentation depth δ/*h*, as a function of σ_f/σ_s and E_f/E_s: (a) soft film on hard substrate; (b) the transition from $\sigma_f < \sigma_s$ to $\sigma_f > \sigma_s$; (c) hard film on soft substrate; and (d) very hard film on soft substrate.

thickness. In that case, the measured hardness H is a combination of film and substrate properties, and the contribution of the substrate becomes more important with increasing indentation depth. Since the substrate is harder than the film, the normalized film hardness increases as the indenter tip is pushed closer to the interface, as shown in Fig. 6(a).

This picture changes dramatically if we consider the results for hard films on soft substrates in Fig. 6(b), where the yield stress mismatch is taken to be 0.4, 1, and 2 with no elastic mismatch. As soon as the yield stress of the film is higher than that of the substrate, the normalized film hardness is no longer constant even for relatively small indentation depths and it decreases quickly with increasing indentation depth. This can be seen even more clearly in Fig. 6(c). The substrate effect is very large for the system of a hard film on a soft substrate. Thus, even an indentation depth as small as 10 to 20% of the film thickness is insufficient to avoid the substrate effect.

The normalized film hardness decreases with increasingly softer substrates [Fig. 6(c)]. This trend reverses, however, when the film is very hard compared to the substrate ($\sigma_f/\sigma_s > 40$). This interesting behavior can be seen in Fig. 6(d), where the normalized film hardness increases with a continued increase of yield stress mismatch. This is so because in the case where the substrate is too soft to support the film, the indentation process is more like a plate bending experiment and the plastic zone size in the film is reduced.

The data in Fig. 6 also indicate that the elastic mismatch E_f/E_s plays a relatively minor role in hardness measurements of thin films. Only for soft films on hard substrates is there a small effect when the indenter approaches the substrate [c.f. Fig. 6(a)]. In most cases, however, the elastic mismatch between film and substrate can be neglected. This can be understood by noting that the load during hardness measurements far exceeds the load for Hertzian indentation and that the deformation is thus fully plastic and finite.[16] Thus, it can be concluded that the elastic mismatch has little importance if one determines the film hardness by measuring the contact area directly. The finite element analysis also shows that the elastic mismatch between film and substrate has similarly little or no effect on the degree of pile-up.

It is also shown in the finite element analysis that the presence of a hard substrate enhances the amount of pile-up for a soft film, as plotted in Fig. 7 for the case where there is no elastic mismatch between film and substrate. Consider the instance of $\sigma_f/\sigma_s = 0.5$ in this figure. Initially, when the indentation depth is small, the plastic pile-up height δ_p in the film is the same as that for an indentation in a bulk material and δ_p changes linearly

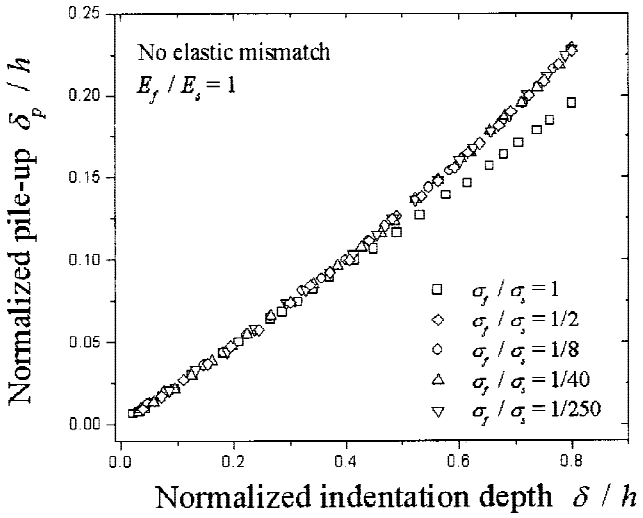

FIG. 7. The normalized relationship between δ/h and δ_p/h: The plastic pile-up in film is enhanced by the presence of the substrate.

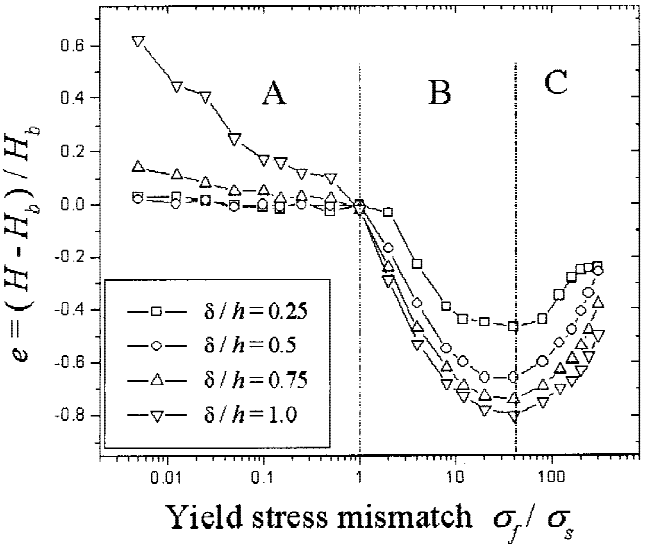

FIG. 8. The relation between the substrate effect factor e and yield stress mismatch σ_f/σ_s for four different indentation depths, δ/h = 0.25, 0.5, 0.75, and 1.

with δ. As the indentation depth increases, however, pile-up for an indentation in a soft film on a hard substrate is larger than for indentations in a bulk material. If the substrate is sufficiently hard that plastic deformation is confined to the film, the degree in pile-up does not change with increasing substrate hardness. This is clearly illustrated in the figure. Once the indenter penetrates the interface, the hard substrate sinks down and slightly reduces the amount of pile-up.[14]

The substrate effect may be further understood by answering the question posed earlier: What does one really measure at a given indentation depth? A substrate effect factor is defined as

$$e = \frac{H - H_b}{H_b} \quad , \tag{10}$$

where H_b is the hardness of a bulk material with the same mechanical properties as the film. The substrate effect factor is the correction factor one needs to take into account when using the relation in Eq. (1), $H = c_b\sigma_f$, to predict the yield stress of the film. The variation of e with σ_f/σ_s is plotted for four different indentation depths in Fig. 8, where we have ignored any effects of E_f/E_s. It is convenient to define three distinct regimes in this nanoindentation hardness map.

Region A is the case of a soft film on hard substrate ($\sigma_f/\sigma_s \leqslant 1$). In this regime, the plastic zone is confined almost exclusively to the film and the hardness determined from Eq. (1) is accurate as long as the indentation depth is less 50% of the film thickness. For deeper indentations, corresponding adjustments should be made to the final value of the film hardness by using Eq. (10) and Fig. 8.

Region B is the case of a hard film on soft substrate ($1 < \sigma_f/\sigma_s \leqslant 40$). In this regime, plasticity is induced mostly in the substrate with only a small plastic region in the film beneath the indenter. Due to the large substrate effect, very shallow indentations are required in order to obtain the intrinsic film hardness. The substrate effect is almost inevitable and the error increases with increasing σ_f/σ_s and indentation depth. This error can be as much as 40% for an indentation depth that is just one quarter of the film thickness. In the worst case, the error may reach 80% when the indentation depth is equal to the film thickness. The transition between regions A and B is very sudden and behaves almost like a step function. Typical plastic zone shape for thin film systems in Regions A and B may be found in Larsen and Simo[12] and will not be redrawn here.

Region C is the case of an ultra-hard film on soft substrate ($\sigma_f/\sigma_s > 40$). The substrate is now fully plastic and unable to support the film from underneath. The plate bending effect becomes significant and further reduces the plastic zone in the film. The contour plot of the von Mises stress field underneath the indenter is given in Fig. 9 for a yield stress mismatch of $\sigma_f/\sigma_s = 60$. The figure shows that the ultra-hard film indeed behaves like a plate clamped around the edge and subjected to bending. As a result, the error of film hardness measurement becomes smaller with increasing hardness mismatch σ_f/σ_s. Note that thin film systems in this regime are quite common when dealing with ceramic coating on soft metal substrates: e.g., Al_2O_3 on Al or diamond on Ti substrates.

Consequently, it is clear that any study of the mechanical properties of thin films using nanoindentation should take into account the fact that film/substrate systems in these three regimes respond in very different ways.

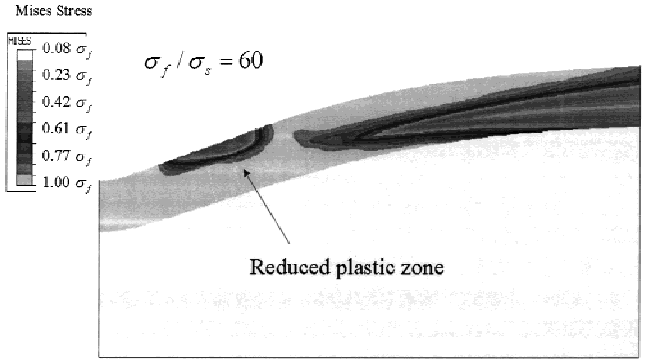

FIG. 9. The computed von Mises stress field beneath the indenter for the case of an ultrahard film deposited on a soft substrate ($\sigma_f/\sigma_s = 60$).

Most indentation techniques use Eq. (2), in one form or another, to determine the indentation modulus of the material under consideration. The indentation modulus of a thin film on a substrate as measured experimentally is of course affected by the elastic properties of the substrate. An approximate analysis by Gao *et al.*[11] yields the following expression for the indentation modulus of a film on a substrate:

$$M = \frac{2\mu_{\text{eff}}}{1 - \nu_{\text{eff}}} \quad , \tag{11}$$

where

$$\begin{cases} \nu_{\text{eff}} = \nu_s + (\nu_f - \nu_s) I_1(h/a) & , \\ \mu_{\text{eff}} = \mu_s + (\mu_f - \mu_s) I_0(h/a) & . \end{cases} \tag{12}$$

Here, μ_f and μ_s are the shear modulus of the film and substrate, respectively. The two functions, I_0 and I_1, are weight functions that reflect the substrate effect and take the following form:

$$\begin{aligned} I_1(\xi) &= \frac{2}{\pi} \arctan\xi + \frac{\xi}{\pi} \ln \frac{1 + \xi^2}{\xi^2} \quad , \\ I_0(\xi) &= \frac{2}{\pi} \arctan\xi + \frac{1}{2\pi(1 - \nu)} \\ &\quad \left[(1 - 2\nu)\xi \ln \frac{1 + \xi^2}{\xi^2} - \frac{\xi}{1 - \xi^2} \right] \quad , \end{aligned} \tag{13}$$

where $\xi = h/a$. Both of these functions approach unity when h/a is very large and the measured indentation modulus is equal to that of the film. On the other hand, when the indentation is deep (h/a is small) both I_0 and I_1 approach zero, indicating that one is indeed measuring the stiffness of the substrate.

Two film systems were chosen for each of the three regimes defined in Fig. 8. Instead of using the approximate formulas by Gao *et al.*,[11] we have used our finite element model to calculate the stiffness weight function $I_0(h/a)$ (with $\nu_f = \nu_s = 0.3$) for each of the film–substrate combinations considered. The weight functions are plotted along with the theoretical result from Gao *et al.*[11] in Fig. 10. The comparison shows that the weight function by Gao *et al.*[11] overestimates the substrate effect when the film is stiffer than the substrate and that the substrate influence is underestimated if the film is more compliant. Figure 10 clearly shows that the weight function $I_0(h/a)$, and thus also the contact stiffness $S(h/a)$, are independent of σ_f/σ_s and that the three different regions defined in the hardness study do not affect the stiffness measurement. The factor that controls the substrate effect in the stiffness measurement is the elastic mismatch E_f/E_s. The stiffness mismatch E_f/E_s in Fig. 10 was taken to be 1.8 and 0.56. These are not extreme values and one would expect the difference in weight function between the stiff film/compliant substrate and the compliant film/stiff substrate to further increase with increasing elastic mismatch.

Since the unloading process is elastic, both film and substrate can be taken as elastic materials without a yield surface in order to investigate the effect of the substrate on the indentation modulus of a thin film. The contact stiffness $dP/d\delta$ thus calculated is equal to the contact stiffness determined from elastic unloading and it can be substituted into Eq. (2) to get the indentation modulus. An analytical solution of this problem, where an elastic bilayer is in contact with a rigid conical indenter, was developed by Yu *et al.*[10] using the integral equation method. In order to examine their results, the normalized indentation load P/P_b is calculated from FEM and drawn as a function of h/a_b in Fig. 11 for two values of elastic mismatch: $E_f/E_s = 0.5$ and $E_f/E_s = 2$. Here, P is the load needed to penetrate to a depth δ into the composite and P_b is the load required to indent to the same depth δ into a homogeneous half-space that is made from the same material as the film. The contact radius a_b of the

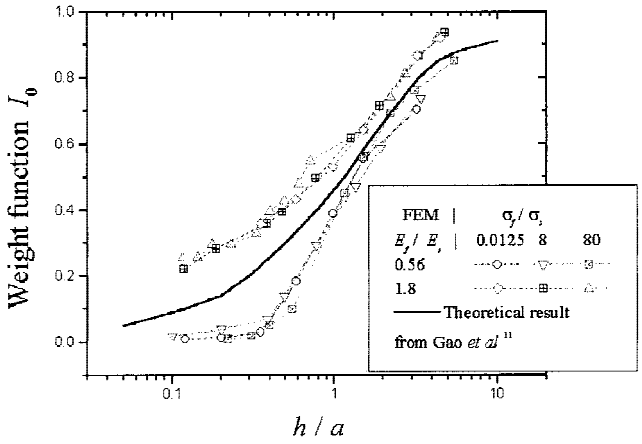

FIG. 10. The comparison between the FEM result and theoretical model by Gao *et al.*[11] of the stiffness weight function $I_0(h/a)$ as a variation of mechanical property mismatches.

homogeneous half-space is also a function of δ. The numerical results are compared with the theoretical results of Yu *et al.*[10] in this plot and show very good agreement.

The analysis by Yu *et al.*[10] is elastic and therefore cannot account for pile-up. Since the unloading process is elastic, however, the contact stiffness must be the same for both elastic and elastic–plastic composites, as long as the contact area is the same.[2] This is so regardless of the fact that the projected contact area in elastic–plastic indentations depends on σ_f/σ_s and that it is very different from that of an elastic indentation to the same load. The analysis by Yu *et al.*[10] was used to calculate the weight function $I_0(h/a)$ for two different values of E_f/E_s. The results are plotted together with the corresponding FEM results in the stiffness map in Fig. 12. The agreement between the theoretical and numerical results is very good. Thus, the solution by Yu *et al.* can be used to analyze data obtained from indentations in very thin films.

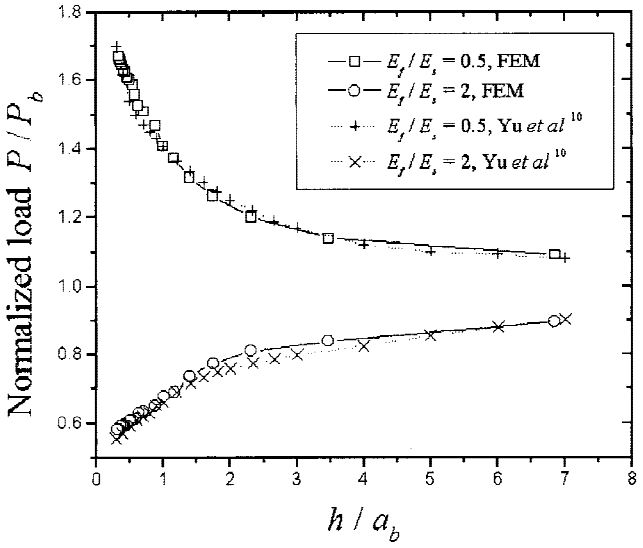

FIG. 11. The variation of the normalized load P/P_b with the normalized contact radius of the homogeneous half-space h/a_b: comparison between the FEM result and theoretical model by Yu *et al.*[10]

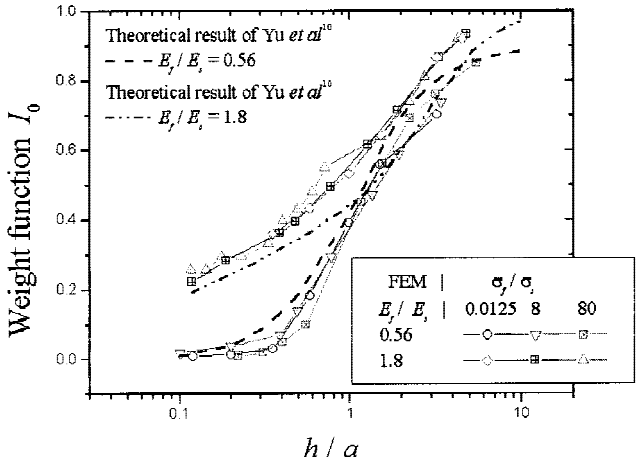

FIG. 12. The comparison between the FEM result and theoretical model by Yu *et al.*[10] of the stiffness weight function $I_0(h/a)$.

As an illustration of how the result of this investigation can be applied to nanoindentation measurements, we propose a new technique for determining the contact area in a nanoindentation experiment. The analytical analysis of Yu *et al.*[10] or our finite element results give the indentation modulus of a thin film on a substrate as a function of the contact area between indenter and film: $M(a/h) = F(A)$. If the Young's moduli of both film and substrate are known, the contact area in an indentation experiment can be determined by solving the following equation for the contact area A:

$$S = \beta\gamma\frac{2}{\sqrt{\pi}}M\left(\frac{a}{h}\right)\sqrt{A} = \beta\gamma\frac{2}{\sqrt{\pi}}F(A)\sqrt{A} \quad . \quad (14)$$

Once the contact area is known, the hardness can be calculated from Eq. (1). The yield stress of the film can be determined iteratively through use of the results in Fig. 8. The advantage of this method of determining the contact area is that unlike the Oliver–Pharr technique it is insensitive to plastic pile-up. It should be noted that this method requires knowledge of Young's modulus of the film. In many cases, the stiffness of a film can be taken equal to that of the bulk material[25–28] and this requirement represents no osbtacle. If the film material is anisotropic, the equivalent polycrystalline modulus can be used to a good approximation.[6,7] If the film is very porous, however, or if the material cannot be obtained in bulk form, its stiffness is generally not known *a priori* and an alternate method such as the Oliver–Pharr technique[2] or direct inspection with a scanning electron microscope or atomic force microscope is required to determine the contact area.

V. CONCLUSIONS

The finite element approach has been used to study the effect of the substrate on the measurement of the mechanical properties of thin films by means of nanoindentation. The following comments are offered in conclusion and may be useful for extracting intrinsic film properties from experimental results, when it is not possible to avoid the substrate effect.

(1) The pile-up height in a bulk material scales linearly with the indentation depth and the ratio δ_p/δ is a function of $E\tan\beta_0/\sigma_y$ with an upper limit of 0.26 and a lower limit of −0.36. The standard expression for the indentation modulus [Eq. (2)] overestimates the stiffness of a bulk material by approximately 8% for a material with Poisson's ratio of 0.3.

(2) For a soft film on a hard substrate ($\sigma_f/\sigma_s \leqslant 1$), the influence of the substrate is not appreciable until $\delta > h/2$. The yield stress of a film, σ_f, can be measured directly

from the relation $H = P/A = c_b\sigma_f$, as long as the indentation depth is less than 50% of the film thickness. Plastic pileup in the film is enhanced by the presence of the hard substrate.

(3) If the yield stress of the film is higher than that of the substrate, plastic deformation of the substrate increases sink-in of the film and the substrate effect is very large. In this case, the substrate effect is inevitable even for indentation depths less than 10 to 20% of film thickness.

(4) When $\sigma_f/\sigma_s > 40$, the film is subjected to plate bending since the film has little support from the yielding substrate underneath. The plastic zone in the film is reduced and the normalized hardness increases with increasing σ_f/σ_s.

(5) A substrate effect factor is defined, which is essentially a correction factor that allows one to determine the yield stress of a film from hardness measurements. A nanoindentation hardness map characterized by the yield stress mismatch σ_f/σ_s is given in Fig. 8. Three distinct regimes are defined on this map, which should be taken into account when measuring the mechanical properties of thin films by nanoindentation.

(6) A stiffness map that quantifies the substrate effect in nanoindentation stiffness measurements as a function of elastic mismatch E_f/E_s was obtained from FEM analysis (Fig. 10), and from an existing theoretical model by Yu *et al.*[10] (Fig. 12). By using the hardness and stiffness maps, a new technique is proposed for measuring the mechanical properties of thin films by nanoindentation if the film stiffness is known *a priori.* This technique is especially useful when it is not possible to avoid substrate effects or pileup.

REFERENCES

1. M.F. Doerner and W.D. Nix, J. Mater. Res. **1,** 601 (1986).
2. W.C. Oliver and G.M. Pharr, J. Mater. Res. **7,** 1564 (1992).
3. T.Y. Tsui, J.J. Vlassak, and W.D. Nix, J. Mater. Res. **14,** 2196 (1999).
4. T.Y. Tsui, J.J. Vlassak, and W.D. Nix, J. Mater. Res. **14,** 2204 (1999).
5. Standard Test Method for Vickers Hardness of Metallic Materials (American Society for Testing and Materials, West Conshohocken, PA, 1987).
6. J.J. Vlassak and W.D. Nix, Philos. Mag. A **67,** 1045 (1993).
7. J.J. Vlassak and W.D. Nix, J. Mech. Phys. Solids **42,** 1223 (1994).
8. K.L. Johnson, *Contact Mechanics* (Cambridge University Press, Cambridge, 1985).
9. R.B. King, Int. J. Solids Struct. **23,** 1657 (1987).
10. H.Y. Yu, S.C. Sanday, and B.B. Rath, J. Mech. Phys. Solids **38,** 745 (1990).
11. H. Gao, C-H. Chiu, and J. Lee, Int. J. Solids Struct. **29,** 2471 (1992).
12. T.A. Larsen and J.C. Simo, J. Mater. Res. **7,** 618 (1992).
13. T.Y. Tsui, W.C. Oliver, and G.M. Pharr, in *Thin Films: Stresses and Mechanical Properties VI,* edited by W.W. Gerberich, H. Gao, J-E. Sundgren, and S.P. Baker (Mater. Res. Soc. Symp. Proc. **436,** Pittsburgh, PA, 1996), p. 207.
14. T.Y. Tsui, C.A. Ross, and G.M. Pharr, in *Materials Reliability in Microelectronics VII,* edited by J.J. Clement, R.R. Keller, K.S. Krisch, J.E. Sanchez, Jr., and Z. Suo (Mater. Res. Soc. Symp. Proc. **473,** Pittsburgh, PA, 1997), p. 51.
15. J.C. Hay and G.M. Pharr, in *Thin Films: Stresses and Mechanical Properties VII,* edited by R.C. Cammarato, M.A. Nastasi, E.P. Busso, and W.C. Oliver (Mater. Res. Soc. Symp. Proc. **505,** Warrendale, PA, 1998), p. 71.
16. A.K. Bhattacharya and W.D. Nix, Int. J. Solids Structures **24,** 1287 (1988).
17. M.R. McGurk, H.W. Chandler, P.C. Twigg, and T.F. Page, Surf. Coat. Technol. **68,** 576 (1994).
18. M.R. McGurk and T.F. Page, Surf. Coat. Technol. **92,** 87 (1997).
19. A.M. Korsunsky, M.R. McGurk, S.J. Bull, and T.F. Page, Surf. Coat. Technol. **99,** 171 (1998).
20. S.D. Mesarovic and N.A. Fleck, Proc. R. Soc. Lond. **455,** 2707 (1999).
21. Hibbit, Karlsson and Sorenson Inc., *ABAQUS Version 5.8 User's Manual* (Pawtucket, RI, 1999).
22. K.W. McElhaney, J.J. Vlassak, and W.D. Nix, J. Mater. Res. **13,** 1300 (1998).
23. J.W. Harding and I.N. Sneddon, Proc. Cambridge Philos. Soc. **14,** 16 (1945).
24. J.C. Hay, A. Bolshakov, and G.M. Pharr, J. Mater. Res. **14,** 2296 (1999).
25. R. Bhadra, M. Grimsditch, I.K. Schuller, and F. Nizzoli, Phys. Rev. **B39,** 12456 (1989).
26. M.G. Beghi, C.E. Bottani, P.M. Ossi, T.A. Lafford, and B.K. Tanner, J. Appl. Phys. **81,** 672 (1997).
27. A.J. Kalkman, A.H. Verbruggen, G.C.A.M. Janssen, and F.H. Groen, Rev. Sci. Instrum. **70,** 4026 (1999).
28. A.J. Kalkman, A.H. Verbruggen, and G.C.A.M. Janssen, Appl. Phys. Lett. **78,** 2673 (2001).